

OPEN

Metabolic Profiling Reveals Biochemical Pathways Responsible for Eelgrass Response to Elevated CO₂ and Temperature

Carmen C. Zayas-Santiago^{1*}, Albert Rivas-Ubach², Li-Jung Kuo³, Nicholas D. Ward^{3,4} & Richard C. Zimmerman¹

As CO₂ levels in Earth's atmosphere and oceans steadily rise, varying organismal responses may produce ecological losers and winners. Increased ocean CO₂ can enhance seagrass productivity and thermal tolerance, providing some compensation for climate warming. However, the metabolic shifts driving the positive response to elevated CO₂ by these important ecosystem engineers remain unknown. We analyzed whole-plant performance and metabolic profiles of two geographically distinct eelgrass (*Zostera marina* L.) populations in response to CO₂ enrichment. In addition to enhancing overall plant size, growth and survival, CO₂ enrichment increased the abundance of Calvin Cycle and nitrogen assimilation metabolites while suppressing the abundance of stress-related metabolites. Overall metabolome differences between populations suggest that some eelgrass phenotypes may be better suited than others to cope with an increasingly hot and sour sea. Our results suggest that seagrass populations will respond variably, but overall positively, to increasing CO₂ concentrations, generating negative feedbacks to climate change.

In addition to being a climate warming greenhouse gas, nearly half of the anthropogenically released carbon dioxide (CO₂) is absorbed by the ocean, eliciting both negative and positive organismal responses to the process known as Ocean Acidification^{1,2}. Benthic calcifiers, including corals and mollusks, are expected to respond negatively as calcification becomes energetically more expensive in an acidified ocean³. However, CO₂ is also a potentially limiting substrate for photosynthesis in both terrestrial and aquatic ecosystems. Terrestrial plants grown under CO₂ enrichment often show increased rates of carbon uptake, sucrose formation, nitrogen and water use efficiencies, dark respiration and growth⁴. Although many marine autotrophs exhibit very little response to CO₂ fertilization⁵, some nitrogen-fixing cyanobacteria⁶, coccolithophores⁷, chlorophytes such as *Caulerpa* spp. and *Ulva* spp.^{8,9}, and especially seagrasses^{10–12} exhibit increased rates of photosynthesis, growth and biomass production under CO₂ enrichment.

Seagrasses are well recognized as important ecosystem engineers¹³ and Blue Carbon reservoirs¹⁴, but their populations are increasingly threatened by anthropogenic degradation of water quality and climate warming¹⁵. Experimental¹⁶ and theoretical¹⁷ evidence indicates that enhanced photosynthesis stimulated by rising CO₂ availability can offset the effects of thermal stress for eelgrass (*Zostera marina* L.); a problem that appears to be increasing with climate warming^{18–20}. Eelgrass, the most widely distributed seagrass species in temperate marine environments of the Northern Hemisphere, persists in geographically isolated populations spanning different thermal environments from the subarctic Bering Sea to the seasonally warm waters of the mid-Atlantic Bight and Mediterranean²¹. This distribution lends eelgrass to be the most extensively studied seagrass species in terms of ecology, physiology and genetics, making it a unique model organism for exploring the impacts of climate change on seagrass ecosystems. In addition, seagrass meadows are among the most productive aquatic habitats in terms

¹Department of Ocean, Earth & Atmospheric Sciences, Old Dominion University, Norfolk, VA, 23429, USA.

²Environmental Molecular Sciences Division, Pacific Northwest National Laboratory, 3335 Innovation Boulevard, Richland, WA, 99352, USA. ³Marine Sciences Laboratory, Pacific Northwest National Laboratory, 1529 W. Sequim Bay Rd., Sequim, WA, 98382, USA. ⁴School of Oceanography, University of Washington, Seattle, WA, 98105, USA.

*email: czayassa@odu.edu

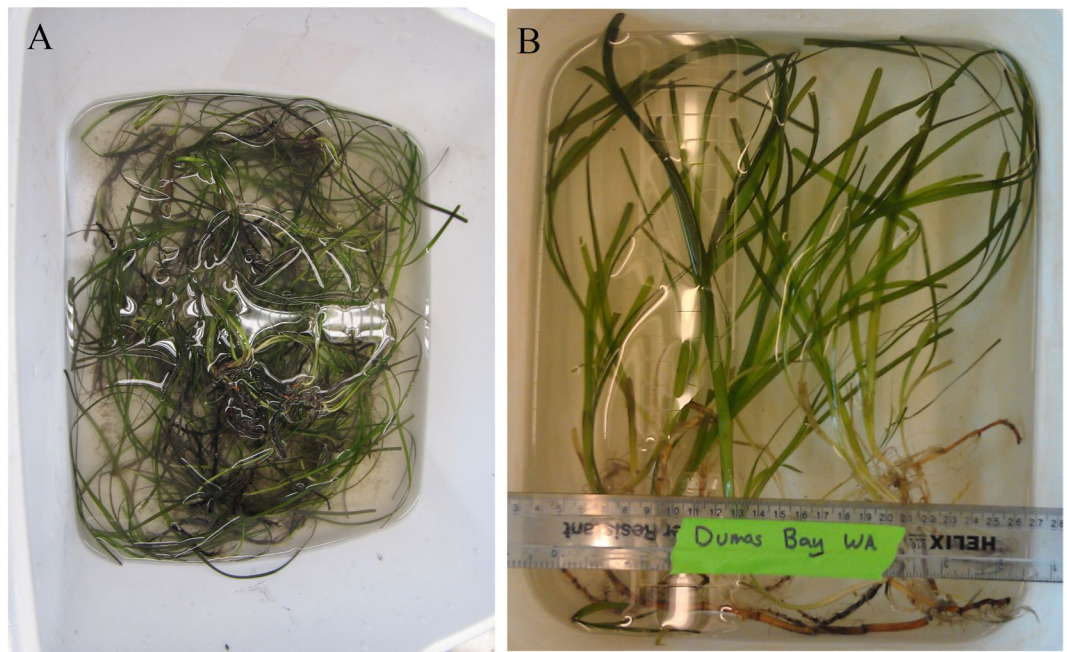


Figure 1. Photographs of eelgrass from (A) South Bay, VA (left) and (B) Dumas Bay, WA (right) showing morphological differences at the time of original collection.

of carbon burial²², suggesting that enhanced seagrass productivity under increasing CO₂ conditions may exert a negative feedback on climate change.

Eelgrass exhibits a wide range of morphological variation throughout its geographic distribution that has been related to local environmental conditions, including substrate type, water depth, temperature, light, nutrient availability and water flow²³ and inherent genetic variation²⁴. These circumstances suggest populations may have had numerous opportunities for genetic adaptation to different environments, making eelgrass an ideal species for exploring the impacts of climate change across geographic regions. However, the degree of morphological and physiological plasticity within geographically isolated populations remains unknown. Heat stress in European populations of *Z. marina* and *Z. noltii* appears to be mediated primarily by its effect on sucrose metabolism²⁵. Consequently, photosynthetic stimulation resulting from CO₂ enrichment increases sucrose formation and should reduce the effects of thermal stress. Prolonged exposure to elevated CO₂ quantitatively enhances leaf photosynthesis, shoot survival, growth and flowering of eelgrass populations from climates characterized by a narrow thermal range (predominantly cool)^{16,26} and a wide thermal range that include stressfully warm summers¹¹, thereby demonstrating that eelgrass productivity and thermal tolerance in the modern-day ocean are strongly mediated by CO₂ availability.

Here we evaluated the physiological and metabolome responses of two distinct eelgrass populations from Puget Sound, Washington and Chesapeake Bay, Virginia, USA that represent contrasting thermal environments. These populations were subjected to an experimental gradient of five CO₂ conditions in an outdoor facility under naturally varying temperature and insolation for one year. Accordingly, we compared the plants physiological processes in response to the environment and characterized the metabolome of the samples at the end of the 1-year exposure period. The metabolome of an organism is considered its chemical phenotype²⁷, as it is the first component responding to external stressors²⁸. The metabolome consists of thousands of low molecular weight metabolites (typically < 800 Da) such as amino acids, organic acids, sugars and phenolic compounds derived from primary and secondary cellular metabolism. This study explored the hypothesis that increased CO₂ availability would stimulate carbon fixation pathways and reduce the biosynthesis of stress-related compounds. Differential responses among populations may help identify heritable traits that facilitate adaptation of eelgrass to a changing climate and improve our predictive capacity for restoring and conserving these important ecosystem engineers.

Morphology and whole plant performance

At the start of this experiment, eelgrass (*Zostera marina* L.) shoots from Puget Sound (Dumas Bay, WA, USA) were significantly longer and wider, reaching up to 1 m in length and 0.3–0.5 cm in width, than eelgrass from the Chesapeake region (South Bay, VA, USA) that grow to about 30 cm in length and 0.1–0.5 cm in width (Fig. 1). CO₂ enrichment yielded strong positive effects on individual shoot size, vegetative shoot numbers (shown as % survival) and sucrose content of both populations during the 12-month experiment (Fig. 2). However, plants from South Bay, VA (SBV) showed larger increases in size compared to those from Dumas Bay, WA (DBW), especially during summer and early fall 2013 (Fig. 2A,B and Table S1). The stimulating effects of CO₂ enrichment on plant size of both populations decreased during the winter period of low light availability and low temperature (Fig. 2A,B white symbols and lines).

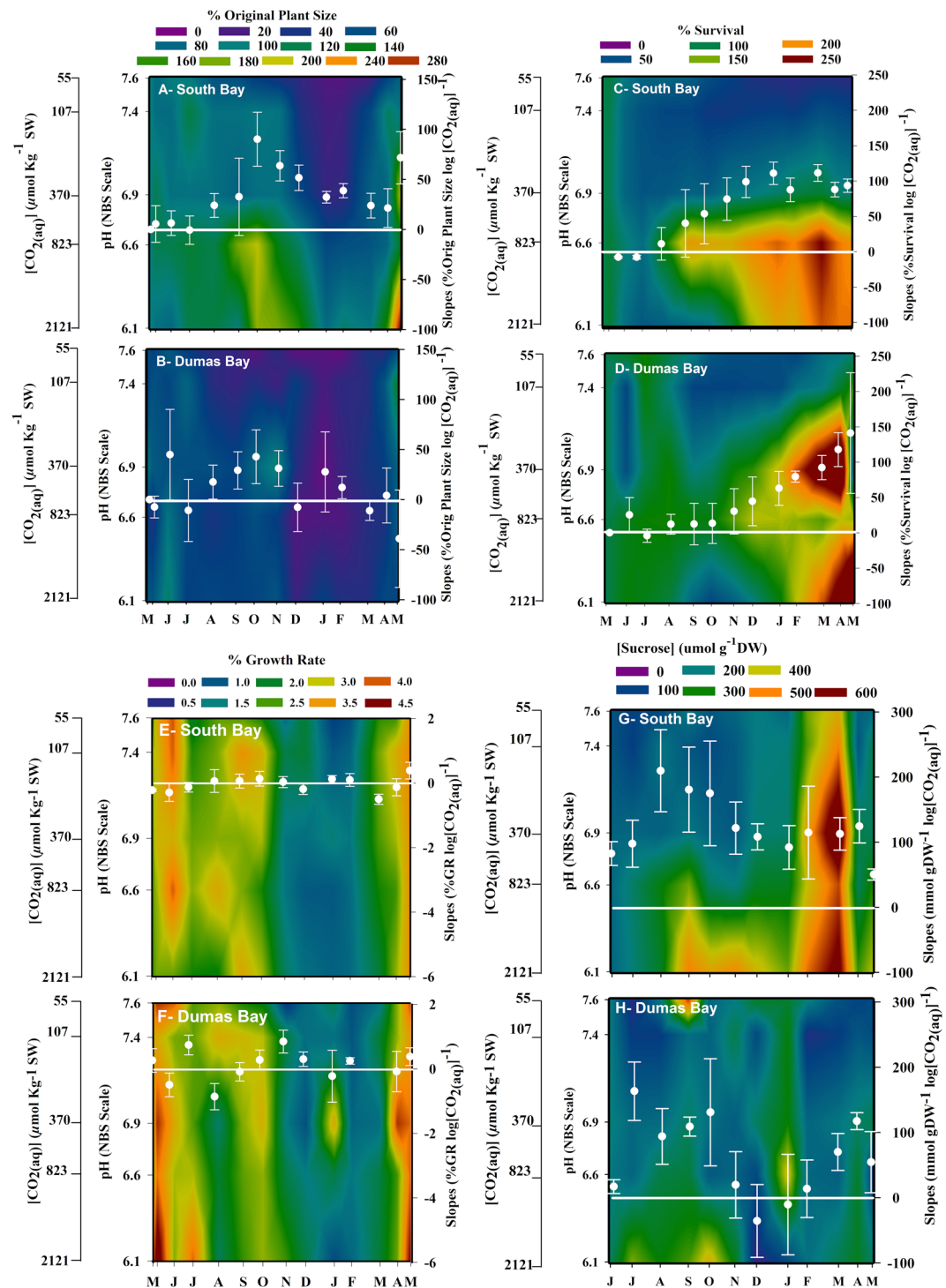


Figure 2. Heat maps showing the responses of South Bay VA and Dumas Bay WA eelgrass populations to $[\text{CO}_2]$ and time. (A,B) Percent plant size. (C,D) Percent shoot survival. (E,F) Relative growth rate. (G,H) Leaf sucrose concentration. Tick marks on the left vertical axis of each plot indicate the mean $[\text{CO}_2]$ for each treatment. White symbols on each plot represent the monthly slope of the response variable vs. $\log [\text{CO}_2]$ derived from linear regression analysis. Error bars represent ± 1 SE of the regression slope. South Bay data adapted from¹¹.

High $[\text{CO}_2]$ stimulated vegetative shoot survival in both eelgrass populations into the fall of 2013 and especially through the winter of 2013–2014 (Fig. 2C,D). However, shoot numbers decreased under ambient $[\text{CO}_2]$ for both eelgrass populations during the summer period of warm ($>25^\circ\text{C}$) water temperature. Shoot losses continued under ambient $[\text{CO}_2]$ as water temperature dropped throughout the fall 2013 and into the winter of 2014. The effect of CO_2 on shoot survival, as indicated by the slope of percent survival vs. $\log [\text{CO}_2]$, was highest from winter (January) to spring (May) 2014 for SBV plants and from early (March) to late (May) spring 2014 for DBW

plants (Fig. 2C,D white symbols and lines, Table S2). At the end of the experiment (May 2014), shoot numbers in the highest CO₂ treatment doubled through vegetative proliferation but less than half originally transplanted shoots survived under ambient [CO₂].

Although plant size and therefore absolute growth rate increased with [CO₂], there was no CO₂ effect on relative growth rate (Fig. 2E,F). Despite CO₂ enrichment, both SBV and DBW populations increased growth rates during summer and early fall of 2013, even when water temperature exceeded the 25 °C threshold for eelgrass heat stress^{18,29,30}. Growth rates of both populations declined during winter period of low light availability and temperature in all CO₂ treatments (Fig. 2E,F) but recovered as temperature and light availability increased during spring 2014. The monthly trends of relative shoot growth (but not absolute growth) were significantly different between populations at different time points. For example, in late summer (August) and late winter (January) SBV showed higher slopes but DBW slopes were higher in fall (November) and winter (December), (Fig. 2E,F, white symbols and lines, Table S3).

Leaf sugar concentrations peaked in all CO₂ treatments for both eelgrass populations in late winter (Fig. 2G,H), when temperature (Fig. S1) and growth were low. Sucrose concentrations of SBV leaves were higher than those from DBW during the whole experiment in high [CO₂]. The monthly slopes of leaf sucrose concentration vs. log [CO₂] were significantly different between eelgrass populations, SBV presented higher slopes (Fig. 2G,H, white symbols and lines, Table S4) in late summer (August), fall (November) and early winter (December).

Metabolomic Response of Eelgrass

Comparison between populations at high and low CO₂. Permutational multivariate analysis of variance (PERMANOVA) of the entire metabolomic fingerprints, including both populations and CO₂, showed overall significant differences between the SBV and DBW populations after 1-year growth in the experimental aquaria (Table S5). However, the interaction between CO₂ treatment and population was not statistically significant ($p = 0.077$) (Table S5), suggesting that both populations showed similar responses to elevated CO₂. Individual one-way ANOVAs for each metabolite detected significant differences ($p < 0.05$) between SBV and DBW plants in the abundance of some primary metabolites (Glycolysis – Krebs – Calvin) across CO₂ treatments (Tables S6 and S7). Principal component analysis (PCA) including the whole eelgrass metabolomic fingerprints clearly clustered the two populations along the first Principal Component Axis 1 (PC1) (Fig. 3A), with CO₂ treatments separated along the PC2 showing differences between plants growing at different [CO₂].

Although CO₂ enhanced growth, survival and thermal tolerance of both eelgrass populations, DBW contained higher abundances of photorespiratory and stress-related compounds in the shikimate pathway than SBV regardless of CO₂ treatments (Fig. 4a,b, Tables S6, S7). Higher abundance of dehydroshikimate (Fig. 4a,b, Tables S6, S7) observed in DBW plants, relative to SBV, may indicate up-regulation of metabolic flux through the shikimate pathway³¹ leading to the synthesis of polyphenols. Stress conditions such as high light and pathogens³², and low CO₂³³ increase the biosynthesis of phenolic compounds in seagrasses. Further, the shikimic intermediates are known to respond to oxidative stress and copper pollution in some macrophytes^{34,35}. On the other hand, SBV plants had higher abundances of α -ketoglutaric acid (TCA Cycle) across CO₂ treatments (Fig. 4a,b, Tables S6, S7). Studies have reported accumulation of α -ketoglutaric acid under oxidative stress in *Z. marina*³⁶ and rice³⁷ and have been suggested as a mitigation mechanisms to manage stressful events limiting the accumulation of pyruvate³⁶.

At high [CO₂], proline and serine were more abundant in DBW eelgrass than in SBV (Fig. 4a, Table S6). Proline is known to aid stress tolerance by acting as a metal chelator, by providing antioxidative defense and as a signaling molecule^{38,39} to control mitochondrial functions and, other developmental processes, and activate gene expression that may facilitate plant recovery from stress⁴⁰. Serine has also been related to stress tolerance (e.g., low temperature and elevated salinity in *Arabidopsis thaliana*⁴¹ and references therein) and is synthesized (i) through the photorespiratory glycolate pathway, (ii) from Calvin Cycle intermediates (the “phosphorylated” pathway) and/or (iii) the glycerate pathway via cytosolic glycolysis⁴². However, high [CO₂] is known to decrease photorespiration in eelgrass⁴³, suggesting that the elevated abundance of serine observed here were likely being driven by non-photorespiratory pathways.

Metabolites involved in biotic/abiotic stress responses were elevated in both populations at low [CO₂] (107 $\mu\text{mol CO}_2\text{-Kg}^{-1}\text{ SW}$). However, the abundance of the photorespiratory metabolites glycerate, glycerate 3-P and succinate semialdehyde (GABA shunt) were higher in DBW leaves than in SBV leaves (Fig. 4b, Table S7). The increase in succinate semialdehyde abundance under low [CO₂] in DBW could represent a potential stress response as the GABA shunt may help prevent the accumulation of reactive oxygen intermediates^{31,32,44,45}. SBV plants growing under low [CO₂] (107 $\mu\text{mol CO}_2\text{-Kg}^{-1}\text{ SW}$) had higher abundance of proline and the sugar alcohol myo-inositol (Fig. 4b, Table S7), the latter are known to generate protein stabilizing osmolytes, such as di-myo-inositol phosphate²⁵ that may help protect this population from heat stress²⁵.

South Bay comparison across CO₂ treatments. The SBV plants were grown across a CO₂ concentration gradient as part of a related experiment¹⁰, enabling us to examine their metabolomic responses to different [CO₂] in some detail. From the over 5,000 detected metabolic features, 455 (9%) increased with [CO₂] and 408 (8.1%) decreased in response to [CO₂]. To date, we identified 131 of the 863 responsive metabolites. Experimental CO₂ enrichment elevated the concentration of intermediates associated with carbon fixation and amino acid synthesis, as well as sucrose, the latter which is consistent with our prior experimental findings^{11,16}. PERMANOVA of the metabolomic fingerprints of SBV plants showed clear statistical differences between CO₂ treatments ($p < 0.05$, Table S8). PCA distinctly clustered SBV plants growing at the highest CO₂ treatment (2121 $\mu\text{mol CO}_2\text{-Kg}^{-1}\text{ SW}$) from the rest along the first principal component axis (PC1), which explains over 30% of the total variability (Fig. 3B), suggesting that plants growing at the highest CO₂ levels experienced the largest metabolic changes. On the other hand, plants growing at ambient CO₂ were separated from the other CO₂ treatments along the

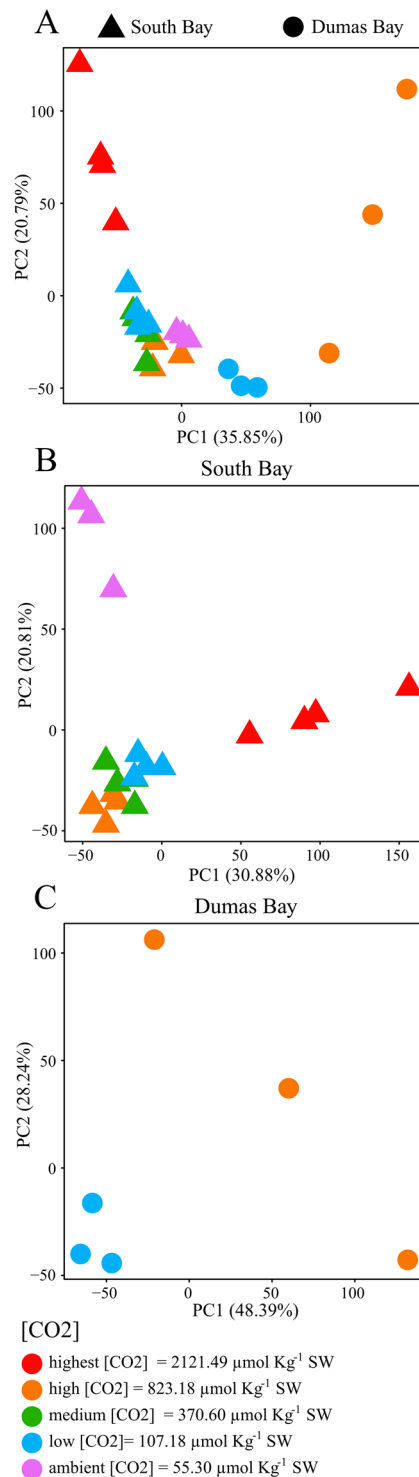


Figure 3. Principal Component Analyses of the metabolome fingerprints of eelgrass leaves from May 2014 growing at different CO₂ concentrations from South Bay, VA (triangles) and Dumas Bay (circles), (A) together, (B) South Bay separately, and (C) Dumas Bay separately. CO₂ treatment is indicated by color.

second principal component axis (PC2). This trend was also observed with the Euclidian distances between the metabolomes of plants growing at higher CO₂ levels (2121, 823, 370, and 107 CO₂·Kg⁻¹ SW) vs. plants growing at ambient [CO₂]. The most dramatic overall metabolome change was detected between the highest (2121 μmol CO₂·Kg⁻¹ SW) and the ambient (55 μmol CO₂·Kg⁻¹ SW) [CO₂] (Fig. 5), consistent with our PCA (Fig. 3B) and with the negative log-linear relationship between [CO₂] and whole plant performance (Fig. 2). SBV plants grown under high [CO₂] had higher abundance of glutamate (Fig. 4c, Table S9) which is involved in N assimilation⁴⁶. In addition, enhancement of gluconate 6-P in SBV plants under high [CO₂] (Fig. 4c, Table S9) suggests activation

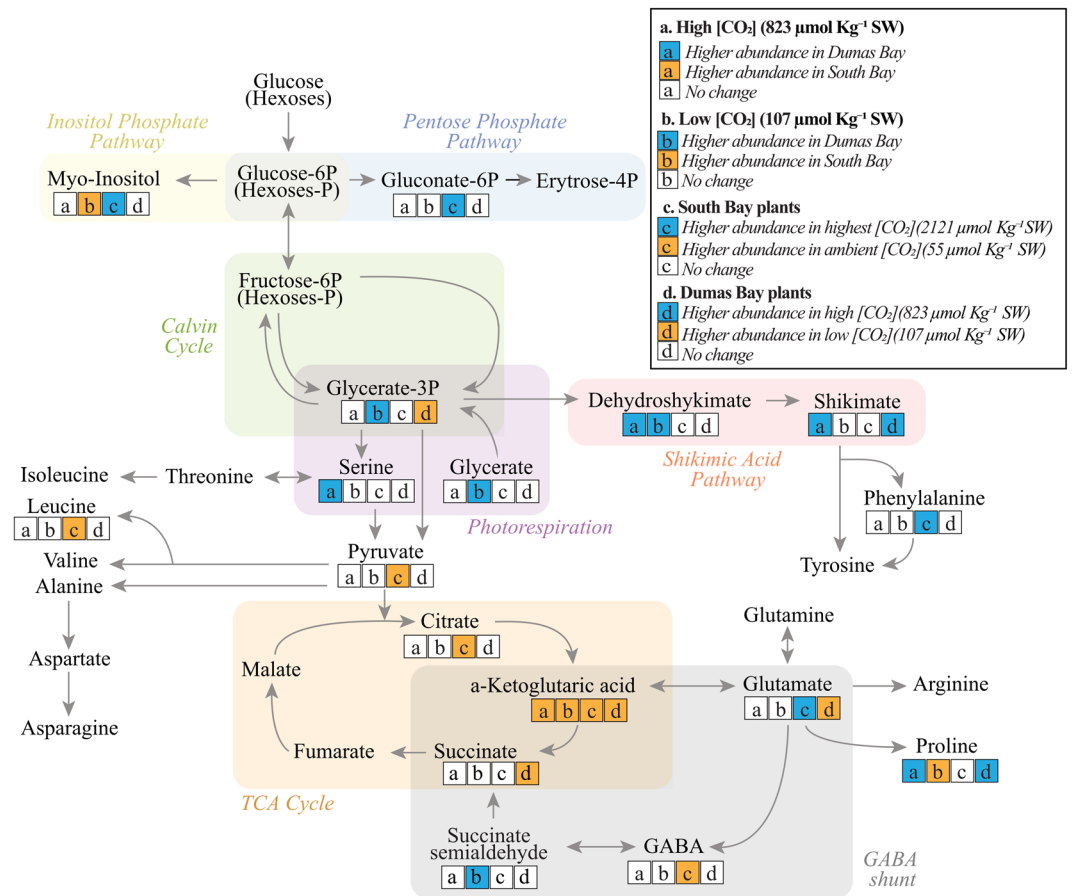


Figure 4. Representation of the main metabolic pathways of *Z. marina* from South Bay VA and Dumas Bay WA in response to high and low CO₂ concentrations. Only identified metabolites are represented in the schema. Significant changes in any of the metabolite comparisons are represented in bold typeface. Colored boxes below metabolite names represent the result of each of the comparisons after one-way ANOVA. Each letter within each box represent a different comparison: (a) South Bay vs. Dumas Bay plants growing at high CO₂ (823 μmol CO₂ kg⁻¹SW). (b) South Bay vs. Dumas Bay plants growing at low CO₂ (107 μmol CO₂ kg⁻¹SW). For a and b, blue and orange colors indicate higher relative abundance in Dumas Bay and South Bay plants, respectively. (c) Highest vs. ambient CO₂ conditions (2121 vs 55 μmol CO₂ kg⁻¹SW) plants from South Bay (d) High vs. low CO₂ conditions (823 vs 107 μmol CO₂ kg⁻¹ SW) plants from Dumas Bay. For c and d, blue and orange color indicate higher relative abundance of metabolites in plants growing at high CO₂ (2121 μmol CO₂ kg⁻¹ SW in c, 823 μmol CO₂ kg⁻¹ SW in d) and ambient or low CO₂ (55 μmol CO₂ kg⁻¹ SW in c, 107 μmol CO₂ kg⁻¹ SW in d), respectively.

of the pentose phosphate pathway⁴⁷ that leads to the synthesis of aromatic amino acids such as phenylalanine; another critical compound in protein synthesis as well as the formation of cell wall components, including lignin⁴⁸. Univariate analyses showed that SBV plants exposed to ambient [CO₂] produced higher abundance of TCA cycle intermediates (Fig. 4c) such as citrate, α-ketoglutarate, pyruvate, and GABA (Table S9). However, we found no differences in leaf dark respiration rates across different [CO₂] treatments or between eelgrass populations when exposed to different temperatures (Fig. S2), suggesting that the increases of TCA Cycle metabolites in plants under ambient CO₂ may have been diverted to other metabolic pathways (e.g. Shikimate) rather than enhancing respiratory ATP production. Although depriving the plant of potential energy for growth, such diversion leads to the synthesis of secondary compounds with diverse physiological roles, such as cell signaling, production of stress-related compounds and the formation of metabolites associated with the biosynthesis of polyphenols⁴⁹. Using a small range of CO₂ conditions, *Cymodocea nodosa* revealed up-regulation of genes coding for respiratory metabolism, increasing energetic demand for biosynthesis and stress-related processes under similar ambient [CO₂] (pH 7.8/[CO₂] 43 μmol Kg⁻¹ SW)⁵⁰. An accurate quantification of this diversion of respiratory intermediates to different pathways may serve as a good proxy for calculating the energetic cost of the physiological stress response to growth and reproductive output.

Dumas Bay comparison between high and low CO₂. For DBW plants, a low number of replicates in some CO₂ treatments did not enable metabolomics analyses across all treatments. However, PERMANOVA did not find overall metabolomic differences between plants growing at low [CO₂] (107 μmol Kg⁻¹ SW) and plants

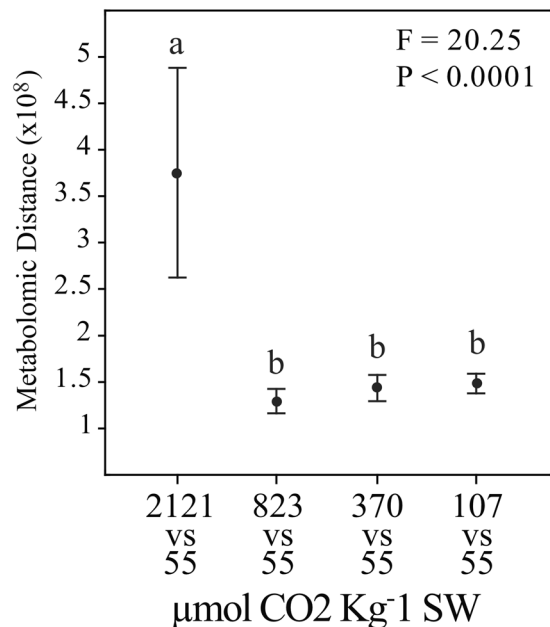


Figure 5. South Bay metabolomic distances (Mean \pm Confidence Intervals 95%) between plants growing at ambient CO₂ (55 $\mu\text{mol CO}_2\cdot\text{kg}^{-1}\text{SW}$) and plants higher CO₂ concentrations (2121, 823, 370, and 107 $\mu\text{mol CO}_2\cdot\text{kg}^{-1}\text{SW}$). Fisher's *F*-statistic and *p* value of the one-way ANOVA comparing the distances are indicated.

under high [CO₂] (823 $\mu\text{mol Kg}^{-1}\text{SW}$) (Table S8). The two clustered in different regions along PC1 (Fig. 3C) but according to individual ANOVAs of the metabolomic fingerprints detected significant changes between CO₂ treatments (Tables S9 and S10). Under low [CO₂] (107 $\mu\text{mol CO}_2\cdot\text{Kg}^{-1}\text{SW}$), DBW plants contained higher levels of α -ketoglutarate, succinate, glutamate and glycerate 3-P (Fig. 4d, Table S10) suggesting activation of the GABA shunt as a way to mitigate stress³⁶. On the other hand, high [CO₂] (823 $\mu\text{mol CO}_2\cdot\text{Kg}^{-1}\text{SW}$) stimulated the abundance of shikimate and proline (Fig. 4d, Table S10) the latter may have increased the thermal tolerance of this population.

Conclusion

Our results revealed that eelgrass populations from two very different thermal environments both exhibited enhanced photosynthetic energy capture, sucrose formation and growth under CO₂ enrichment that increased thermal tolerance, potentially counteracting some climate warming impacts on this foundational species. Both populations exhibited positive whole plant responses to CO₂ in terms of leaf sucrose, leaf growth, and shoot numbers, but metabolite profiles hint at important genetic differences between these populations. Metabolomic analyses suggest that stress diverts the flow of photosynthates from growth and energy (ATP) production to non-anabolic intermediates that may help (i) elucidate important mechanisms responsible for stress tolerance and (ii) quantify the energetic cost of the stress response.

Although the differences in metabolite pools observed here in response to different [CO₂] point to shifts in the activities of metabolic pathways leading to whole plant responses to potential climate forcing, we note that metabolite pool sizes alone are insufficient to fully understand the physiological basis for whole-plant responses to climate-driven environmental change. In addition to making more detailed analyses of metabolite change over time, analyses of changes in the proteome and transcriptome will be necessary to fully understand key genomic functions and metabolic pathways, and those analyses are currently under way. However, the metabolite profiles generated here, in combination with analysis of whole-plant performance, provide a force multiplier for translating 'omic' approaches into a predictive understanding of the physiological response of seagrasses to an increasingly hot and sour sea, and the potential for populations to adapt to new environments. Such knowledge will help predict earth system interactions in the context of global cycles and help inform best practices for seagrass restoration.

Methods

Plant collection. Eelgrass shoots with at least 5 rhizomatous internodes and roots were collected by hand from populations in (i) South Bay, Virginia, near the southern limit of their distribution in the Western Atlantic that experience a large seasonal temperature range and (ii) Dumas Bay in southern Puget Sound, WA that are less vulnerable to summertime thermal stress (Fig. S1). Shoots were carefully uprooted by hand, washed free of all sediment and transported to the experimental growth facility at the Virginia Aquarium & Marine Science Center, Virginia Beach, VA. Shoots from Dumas Bay, WA were packed in paper towels moistened with seawater, shipped overnight to VA and immediately transplanted into the experimental facility.

Experimental facility. Eelgrass shoots were grown in fully replicated aquaria using the climate change experimental facility at the Virginia Aquarium & Marine Science Center¹¹. The experimental system consisted of 20 outdoor aquaria plumbed with running water (10 turnovers/day) pumped from the adjacent Owls Creek estuary (Fig S3). Shoots were transplanted into rectangular fiberglass-reinforced plastic containers (0.04 m³ volume, 0.075 m² surface area) filled with clean intertidal sand and placed in each aquarium. CO₂ concentrations were manipulated using beverage-grade CO₂ delivered through pH-controlled CO₂ bubblers to maintain aquaria at five CO₂ concentrations ranging from ambient (55 μmol CO₂ Kg⁻¹ SW, pH ~8.0) to 2121 μmol CO₂ Kg⁻¹ SW (pH 6) that encompasses a 200-year projection for CO₂ availability and yielded a 3-fold gradient in light-saturated photosynthesis for the duration of the experiment^{10,51}.

Whole plant performance. Shoot counts, size, growth, and sucrose content of leaf tissues were measured each month to track the temporal changes across the CO₂ treatment range as previously described¹¹.

Metabolic profiling. *Tissue collection, storage and processing.* One leaf sample (2nd youngest leaf) was collected monthly at random from each plastic container (three plastic containers for SBV and one for DBV in every aquarium). Epiphytes were removed by gently scraping each leaf with a clean razor blade, followed by a brief rinse in 0.2 μm-filtered seawater. The clean leaves were patted dry with a tissue, flash frozen in liquid nitrogen and stored at -80 °C. Samples collected in May 2014 used for the metabolomics analyses performed here were lyophilized for at least 48 h and powdered using a ball mill. The powdered samples were incubated in methanol/deionized water (4/1 v/v) at 10 °C on an orbital shaker (1 h), followed by gentle sonication for 2 min using a Branson ultrasonic cleaner (40 kHz). The extracts were centrifuged and the supernatants transferred to pre-combusted (450 °C for 8 h) amber glass vials for metabolite analysis. Three solvent-only vials were prepared using only methanol/deionized water (no plant material) processed as above.

GC-MS analyses of plant tissues. 50 μL of eelgrass extract from each sample was dried and subsequently derivatized in two different steps⁵². First, compounds were derivatized to a trimethylsilyl ester form using methoxyamine in pyridine solution (30 mg/mL). 20 μL of methoxyamine solution was added to each dried extract and samples were incubated at 37 °C for 90 min in a Thermomixer operating at 1,200 rpm. Later, amine, carboxyl and hydroxyl groups were derivatized using 80 μL of MSTFA (N-Methyl-N-(trimethylsilyl) trifluoroacetamide), subsequently incubated at 37 °C for 30 min at 1,200 rpm. After derivatization, all extracts were vortexed for 10 s and centrifuged at 2,750 × g for 5 minutes and supernatants were used for GC-MS analyses.

GC-MS analyses were performed using an Agilent GC 7890A equipped with an HP-5MS column (30 m × 0.25 mm × 0.25 μm; Agilent Technologies) coupled to a MSD 5975C mass spectrometer (Agilent Technologies, Santa Clara, CA). The injection port temperature was 250 °C. Injection volume was set at 10 μL and split-less. The column was maintained at 60 °C for 1 min and then increased at a rate of 10 °C min⁻¹ to 325 °C during the following 26.5 min and held for 10 min. Experimental blanks from the solvent-only vials were injected every 15 samples and a mixture of fatty acid methyl esters (FAMES; C8-C28) was analyzed at the beginning of the sequence to calculate retention indices (RI).

Chromatograms were deconvoluted and aligned according to the RI that were calculated from the FAMES mixture run at the beginning of the sequence. Metabolite identification was conducted by matching MS spectra and RI to an updated version of FiehnLib⁵³. Assigned metabolites were subsequently validated using fragmentation spectra from NIST14 GC-MS library. Parameters used in the Metabolite detector are shown in Table S11. Metabolite matching information in GC-MS is shown in Table S12 and more details as previously described⁵².

LC-MS analyses of plant tissues. LC-MS analyses were performed using a Vanquish ultra-high pressure liquid chromatography system (UHPLC) coupled to an LTQ Orbitrap Velos mass spectrometer equipped with heated electrospray ionization (HESI) source (Thermo Fisher Scientific, Waltham, Massachusetts, USA). Chromatography was performed with a Hypersil gold C18 reversed-phase column (150 × 2.1 mm, 3 μm particle size; Thermo Scientific, Waltham, Massachusetts, USA) operating at 30 °C. Mobile phases consisted of 0.1% formic acid in water (A) and 0.1% formic acid in acetonitrile/water (90:10) (B). The injection volume was 5 μL and flow rate was constant at 0.3 mL min⁻¹. The elution gradient started at 90% A (10% B) constant for 5 min and then linearly changed to 10% A (90% B) during the following 15 min. Those conditions were held for 2 min before the initial conditions were recovered during the subsequent 2 min and the column was washed and stabilized for 11 min. All samples were injected in both negative (-) and positive (+) ionization modes. The MS operated at a resolution of 60,000 in Fourier Transform Mass Spectrometry (FTMS) full-scan mode measuring a mass range of 50 to 1000 m/z. Experimental blanks from the solvent-only vials were injected every 15 samples. Details on the MS was previously described⁵⁴.

LC-MS negative and positive chromatograms were separately processed with MZmine 2.26⁵⁵. Chromatograms were baseline corrected, deconvoluted, aligned and metabolic features were assigned to metabolites according to retention time (RT) and exact mass of standard compounds included in our in-house library (second level identification according to Sumner *et al.*^{56,57}). The parameters used for the extraction of the metabolic fingerprints are given in Table S13. Metabolite matching information in LC-MS is shown in Table S14.

Statistical analysis. *Whole plant performance.* Within-aquarium replicate measures of each performance property were combined each month to generate statistically independent means for each aquarium (without error), resulting in statistically independent replicate measurements for each CO₂ treatment each month. Consequently, statistical significance of treatment effects was determined using a repeated-measures ANCOVA implemented in the mixed model analysis of the linear mixed model component of IBM SPSS Statistics 22 using population and month as the fixed factors (within subjects) and log CO₂ as the covariate (between subjects). The

time series observations were treated as repeated subjects for each measured parameter. All error terms were expressed as standard errors unless otherwise noted.

Metabolomics. The final metabolomic dataset was composed of two categorical factors (Population and CO₂ treatment) and 5757 continuous variables (metabolomic features), including 133 metabolites identified by our LC-MS and GC-MS compound libraries. Full factorial PERMANOVAs (Population + CO₂ + Population × CO₂) were performed to test for overall metabolomic differences between populations and CO₂ levels. Both populations were exposed to all five [CO₂] levels however for the metabolomics analyses the DBW population had a low number of replicates in some CO₂ treatments constraining the metabolomics analyses across all treatments. Therefore, we only used two levels of CO₂ for both populations (823 and 107 μmol CO₂·kg⁻¹ SW) to be consistent with both populations for the full PERMANOVA model. Additional PERMANOVAs were performed to test for overall differences for CO₂ treatments within each eelgrass population. All PERMANOVAs were computed using the Euclidean distance and 10,000 permutations. In addition, one-way ANOVAs were performed on individual metabolic features contrasting (i) DBW vs. SBV plants at high [CO₂] (823 μmol CO₂ kg⁻¹ SW), (ii) DBW vs. SBV plants at low [CO₂] (107 μmol CO₂ kg⁻¹ SW), (iii) highest [CO₂] (2121 μmol CO₂ kgSW⁻¹) vs. ambient [CO₂] (55 μmol CO₂ kgSW⁻¹) for SBV plants, and (iv) high [CO₂] (823 μmol CO₂ kgSW⁻¹) vs. low [CO₂] (107 μmol CO₂ kgSW⁻¹) for DBW plants.

The datasets (SBV + DBW, SBV alone, and DBW alone) were subsequently subjected to principal component analysis (PCA) to visualize the overall metabolomic variability of the study cases along the two axes explaining most variability (principal component (PC) 1 and PC2).

The Euclidean distances (metabolomic distances) between plants growing at ambient CO₂ (55 μmol CO₂·kg⁻¹SW) and plants at higher CO₂ concentrations (2121, 823, 370, and 107 μmol CO₂ kg⁻¹SW) were calculated using the entire metabolomic fingerprints. Those distances were posteriorly submitted to one-way ANOVAs followed by Tukey HSD post-hoc test to understand which [CO₂] had a higher response in comparison to ambient [CO₂]. Pearson correlation coefficients (*r*) between CO₂ gradient and individual metabolic features for SBV plants were calculated.

All statistical analyses for metabolomics were performed in R version 3.6.1⁵⁸. PERMANOVAs were performed using the *adonis* function from the package “vegan”⁵⁹. One-way ANOVAs and Euclidian distances were calculated with the functions *aov* and *dist*, respectively, included in the package “stats”⁵⁸. Tukey HSD post hoc tests were conducted using the *HSD.test* function from the *agricolae* package⁶⁰. All PCAs were performed using the function *PCA* found in 2323 “FactoMineR” package⁶¹. For PCAs, missing data were previously imputed using the function *imputePCA* from “missMDA” package⁶².

Data availability

Whole-plant metabolic data are available from BCO-DMO (Principal Investigator Richard Zimmerman, Project: Impact of Climate Warming and Ocean Carbonation on Eelgrass (*Zostera marina* L.). Metabolomics data are also available in the Supporting Information for this manuscript.

Received: 24 May 2019; Accepted: 25 February 2020;

Published online: 13 March 2020

References

1. Doney, S. C., Fabry, V. J., Feely, R. A. & Kleypas, J. A. Ocean acidification: the other CO₂ problem. *Annual Review of Marine Science* **1**, 23, <https://doi.org/10.1146/annurev.marine.010908.163834> (2009).
2. Penuelas, J. & Sardans, J. Ecological metabolomics. *Chemistry and Ecology* **25**, 305–309 (2009).
3. Kleypas, J. *et al.* Impacts of ocean acidification on coral reefs and other marine calcifiers: a guide for future research. *Report of a workshop held 18–20 April 2005 St. Petersburg, FL sponsored by NSF, NOAA, and the U.S. Geological Survey* **18**, 88 (2006).
4. Leakey, A. D. *et al.* Elevated CO₂ effects on plant carbon, nitrogen, and water relations: six important lessons from FACE. *Journal of Experimental Botany* **60**, 2859–2876 (2009).
5. Mackey, K. R., Morris, J. J., Morel, F. M. & Kranz, S. A. Response of photosynthesis to ocean acidification. *Oceanography* **28**, 74–91 (2015).
6. Hutchins, D. *et al.* CO₂ control of Trichodesmium N₂ fixation, photosynthesis, growth rates, and elemental ratios: Implications for past, present, and future ocean biogeochemistry. *Limnology and Oceanography* **52**, 1293–1304 (2007).
7. Rivero-Calle, S., Gnanadesikan, A., Del Castillo, C. E., Balch, W. M. & Guikema, S. D. Multidecadal increase in North Atlantic coccolithophores and the potential role of rising CO₂. *Science* **350**, 1533–1537 (2015).
8. Beer, S. Mechanisms of inorganic carbon acquisition in marine microalgae (with special reference to the Chlorophyta). *Progress in Phycological Research* **10**, 179–179 (1994).
9. Hall-Spencer, J. M. *et al.* Volcanic carbon dioxide vents show ecosystem effects of ocean acidification. *Nature* **454**, 96 (2008).
10. Invers, O., Zimmerman, R., Alberte, R., Perez, M. & Romero, J. Inorganic carbon sources for seagrass photosynthesis: an experimental evaluation for bicarbonate use in temperate species. *The Journal of Experimental Marine Biology and Ecology* **265**, 203–217 (2001).
11. Zimmerman, R. C. *et al.* Experimental impacts of climate warming and ocean carbonation on eelgrass *Zostera marina*. *Marine Ecology Progress Series* **566**, 1–15 (2017).
12. Jiang, Z. J., Huang, X. P. & Zhang, J. P. Effects of CO₂ Enrichment on Photosynthesis, Growth, and Biochemical Composition of Seagrass *Thalassia hemprichii* (Ehrenb.) Aschers. *Journal of Integrative Plant Biology* **52**, 904–913, <https://doi.org/10.1111/j.1744-7909.2010.00991.x> (2010).
13. Jones, C. G., Lawton, J. H. & Shachak, M. in *Ecosystem management* 130–147 (Springer, 1994).
14. Macreadie, P. I., Serrano, O., Maher, D. T., Duarte, C. M. & Beardall, J. Addressing calcium carbonate cycling in blue carbon accounting. *Limnology and Oceanography Letters* **2**, 195–201 (2017).
15. Orth, R. J. *et al.* A global crisis for seagrass ecosystems. *Bioscience* **56**, 987–996 (2006).
16. Palacios, S. L. & Zimmerman, R. C. Response of eelgrass *Zostera marina* to CO₂ enrichment: possible impacts of climate change and potential for remediation of coastal habitats. *Marine Ecology Progress Series* **344**, 1 (2007).
17. Zimmerman, R. C., Hill, V. J. & Gallegos, C. L. Predicting effects of ocean warming, acidification, and water quality on Chesapeake region eelgrass. *Limnology and Oceanography* **60**, 1781–1804, <https://doi.org/10.1002/lno.10139> (2015).

18. Moore, K. A. & Jarvis, J. C. Environmental Factors Affecting Recent Summertime Eelgrass Diebacks in the Lower Chesapeake Bay: Implications for Long-term Persistence. *Journal of Coastal Research*, 135–147 (2008).
19. Winters, G., Nelle, P., Fricke, B., Rauch, G. & Reusch, T. B. Effects of a simulated heat wave on photophysiology and gene expression of high- and low-latitude populations of *Zostera marina*. *Marine Ecology Progress Series* **435**, 83–95 (2011).
20. Thom, R., Southard, S. & Borde, A. Climate-linked mechanisms driving spatial and temporal variation in eelgrass (*Zostera marina* L.) Growth and assemblage structure in Pacific Northwest estuaries, USA. *Journal of Coastal Research* **68**, 1–11 (2014).
21. Moore, K. & Short, F. In *Seagrasses: Biology, Ecology and Conservation* (eds Anthony W.D. Larkum, Robert J. Orth, & Carlos M. Duarte) Ch. 16, 361–386 (Springer, 2006).
22. Mcleod, E. *et al.* A blueprint for blue carbon: toward an improved understanding of the role of vegetated coastal habitats in sequestering CO₂. *Frontiers in Ecology and the Environment* **9**, 552–560 (2011).
23. Holmer, M., Baden, S., Boström, C. & Moksnes, P.-O. Regional variation in eelgrass (*Zostera marina*) morphology, production and stable sulfur isotopic composition along the Baltic Sea and Skagerrak coasts. *Aquatic Botany* **91**, 303–310 (2009).
24. Hughes, A. R., Stachowicz, J. J. & Williams, S. L. Morphological and physiological variation among seagrass (*Zostera marina*) genotypes. *Oecologia* **159**, 725–733 (2009).
25. Gu, J. *et al.* Identifying core features of adaptive metabolic mechanisms for chronic heat stress attenuation contributing to systems robustness. *Integrative Biology* **4**, 480–493 (2012).
26. Zimmerman, R. C., Kohrs, D. G., Steller, D. L. & Alberte, R. S. Impacts of CO₂ enrichment on productivity and light requirements of eelgrass. *Plant Physiology* **115**, 599–607 (1997).
27. Fiehn, O. Metabolomics – the link between genotypes and phenotypes. *Plant Molecular Biology* **48**, 155–171, <https://doi.org/10.1023/a:1013713905833> (2002).
28. Gargallo-Garriga, A. *et al.* Root exudate metabolomes change under drought and show limited capacity for recovery. *Scientific Reports* **8**, 12696, <https://doi.org/10.1038/s41598-018-30150-0> (2018).
29. Zimmerman, R. C., Smith, R. D. & Alberte, R. S. Thermal acclimation and whole-plant carbon balance in *Zostera marina* L. (eelgrass). *Journal of Experimental Marine Biology and Ecology* **130**, 93–109, [https://doi.org/10.1016/0022-0981\(89\)90197-4](https://doi.org/10.1016/0022-0981(89)90197-4) (1989).
30. Thayer, G. W., Wolfe, D. A. & Williams, R. B. The Impact of Man on Seagrass Systems. *American Scientist*, 288–296 (1975).
31. Singh, S. A. & Christendat, D. Structure of Arabidopsis Dehydroquinase Dehydratase-Shikimate Dehydrogenase and Implications for Metabolic Channeling in the Shikimate Pathway. *Biochemistry* **45**, 7787–7796, <https://doi.org/10.1021/bi060366+> (2006).
32. Vergeer, L. H. T., Aarts, T. L. & de Groot, J. D. The ‘wasting disease’ and the effect of abiotic factors (light intensity, temperature, salinity) and infection with *Labyrinthula zosterae* on the phenolic content of *Zostera marina* shoots. *Aquatic Botany* **52**, 35–44, [https://doi.org/10.1016/0304-3770\(95\)00480-N](https://doi.org/10.1016/0304-3770(95)00480-N) (1995).
33. Arnold, T. *et al.* Ocean acidification and the loss of phenolic substances in marine plants. *PLoS One* **7**, e35107, <https://doi.org/10.1371/journal.pone.0035107> (2012).
34. Zou, H.-X. *et al.* Behavior of the Edible Seaweed *Sargassum fusiforme* to Copper Pollution: Short-Term Acclimation and Long-Term Adaptation. *Plos One* **9**, e101960, <https://doi.org/10.1371/journal.pone.0101960> (2014).
35. Kumari, P., Reddy, C. R. K. & Jha, B. Methyl Jasmonate-Induced Lipidomic and Biochemical Alterations in the Intertidal Macroalga *Gracilaria dura* (Gracilariaceae, Rhodophyta). *Plant and Cell Physiology* **56**, 1877–1889, <https://doi.org/10.1093/pcp/pcv115> (2015).
36. Hasler-Sheetal, H., Fragner, L., Holmer, M. & Weckwerth, W. Diurnal effects of anoxia on the metabolome of the seagrass *Zostera marina*. *Metabolomics* **11**, 1208–1218, <https://doi.org/10.1007/s11306-015-0776-9> (2015).
37. Miro, B. & Ismail, A. Tolerance of anaerobic conditions caused by flooding during germination and early growth in rice (*Oryza sativa* L.). *Frontiers in Plant Science* **4**, <https://doi.org/10.3389/fpls.2013.00269> (2013).
38. Verbruggen, N. & Hermans, C. Proline accumulation in plants: a review. *Amino Acids* **35**, 753–759, <https://doi.org/10.1007/s00726-008-0061-6> (2008).
39. Hayat, S. *et al.* Role of proline under changing environments. *Plant Signaling & Behavior* **7**, 1456–1466, <https://doi.org/10.4161/psb.21949> (2012).
40. Szabados, L. & Savouré, A. Proline: a multifunctional amino acid. *Trends in Plant Science* **15**, 89–97, <https://doi.org/10.1016/j.tplants.2009.11.009> (2010).
41. Ho, C.-L. & Saito, K. Molecular biology of the plastidic phosphorylated serine biosynthetic pathway in *Arabidopsis thaliana*. *Amino Acids* **20**, 243–259, <https://doi.org/10.1007/s007260170042> (2001).
42. Bourguignon J, Rebéillé F & Douce R. In *Plant amino acids: Biochemistry & biotechnology* (ed Singh BK) 111–146 (Marcell Dekker, Inc, 1998).
43. Celebi, B. *Potential impacts of Climate Change on photochemistry in Zostera marina* L. PhD thesis, Old Dominion University, Norfolk, VA, (2016).
44. Shelp, B. J., Bown, A. W. & McLean, M. D. Metabolism and functions of gamma-aminobutyric acid. *Trends in Plant Science* **4**, 446–452, [https://doi.org/10.1016/S1360-1385\(99\)01486-7](https://doi.org/10.1016/S1360-1385(99)01486-7) (1999).
45. Bouché, N., Fait, A., Bouchez, D., Möller, S. G. & Fromm, H. Mitochondrial succinic-semialdehyde dehydrogenase of the γ -aminobutyrate shunt is required to restrict levels of reactive oxygen intermediates in plants. *Proceedings of the National Academy of Sciences* **100**, 6843–6848, <https://doi.org/10.1073/pnas.1037532100> (2003).
46. Forde, B. G. & Lea, P. J. Glutamate in plants: metabolism, regulation, and signalling. *Journal of Experimental Botany* **58**, 2339–2358, <https://doi.org/10.1093/jxb/erm121> (2007).
47. Tabita, F. R. & McFadden, B. A. Regulation of ribulose-1,5-diphosphate carboxylase by 6-phospho-D-gluconate. *Biochemical and Biophysical Research Communications* **48**, 1153–1159, [https://doi.org/10.1016/0006-291X\(72\)90831-5](https://doi.org/10.1016/0006-291X(72)90831-5) (1972).
48. Bonawitz, N. D. & Chapple, C. The genetics of lignin biosynthesis: connecting genotype to phenotype. *Annual review of genetics* **44**, 337–363, <https://doi.org/10.1146/annurev-genet-102209-163508> (2010).
49. Weaver, L. M. & Herrmann, K. M. Dynamics of the shikimate pathway in plants. *Trends in Plant Science* **2**, 346–351, [https://doi.org/10.1016/S1360-1385\(97\)84622-5](https://doi.org/10.1016/S1360-1385(97)84622-5) (1997).
50. Ruocco, M. *et al.* Genomewide transcriptional reprogramming in the seagrass *Cymodocea nodosa* under experimental ocean acidification. *Molecular Ecology*, n/a–n/a, <https://doi.org/10.1111/mec.14204> (2017).
51. Cottingham, K. L., Lennon, J. T. & Brown, B. L. Knowing when to draw the line: designing more informative ecological experiments. *Frontiers in Ecology and the Environment* **3**, 145–152 (2005).
52. Kim, Y.-M. *et al.* Diel metabolomics analysis of a hot spring chlorophototrophic microbial mat leads to new hypotheses of community member metabolisms. *Frontiers in Microbiology* **6**, 209 (2015).
53. Kind, T. *et al.* FiehnLib: mass spectral and retention index libraries for metabolomics based on quadrupole and time-of-flight gas chromatography/mass spectrometry. *Analytical Chemistry* **81**, 10038–10048 (2009).
54. Rivas-Ubach, A. *et al.* Similar local, but different systemic, metabolomic responses of closely related pine subspecies to folivory by caterpillars of the processionary moth. *Plant Biology* **18**, 484–494, <https://doi.org/10.1111/plb.12422> (2016).
55. Pluskal, T., Castillo, S., Villar-Briones, A. & Orešič, M. MZmine 2: modular framework for processing, visualizing, and analyzing mass spectrometry-based molecular profile data. *BMC bioinformatics* **11**, 395 (2010).
56. Sumner, L. W. *et al.* Proposed minimum reporting standards for chemical analysis. *Metabolomics* **3**, 211–221 (2007).
57. Myers, O. D., Sumner, S. J., Li, S., Barnes, S. & Du, X. One Step Forward for Reducing False Positive and False Negative Compound Identifications from Mass Spectrometry Metabolomics Data: New Algorithms for Constructing Extracted Ion Chromatograms and Detecting Chromatographic Peaks. *Analytical Chemistry* **89**, 8696–8703, <https://doi.org/10.1021/acs.analchem.7b00947> (2017).

58. Team, R. C. R Core Team (2019). R: A language and environment for statistical computing. *R Found. Stat. Comput. Vienna, Austria*. URL <http://www.R-project.org/>, page R Foundation for Statistical Computing (2019).
59. Oksanen, J., et al. *Vegan: Community Ecology Package*. R package version 2.3.2. *R package version 2.3.2*. (2013).
60. Mendiburu, F. *agricolae: Statistical Procedures for Agricultural Research*. R package version 1.2-3. (2015).
61. Husson, F., Josse, J., Le, S. & Mazet, J. Multivariate exploratory data analysis and data mining. *R Package* (2016).
62. Josse, J. & Husson, F. *missMDA: a package for handling missing values in multivariate data analysis*. *Journal of Statistical Software* **70**, 1–31 (2016).

Acknowledgements

We thank V. Hill, D. Ruble, B. Celebi and M. Jinuntuya for maintenance of the eelgrass experiments and assistance with collection of the leaf samples. Mark Swingle, Sean Bourgeois and Charles Jourdant of the Virginia Aquarium provided operational maintenance of the experimental system. Financial support for the experimental portion of this research was provided by grants from the National Science Foundation (OCE-1061823 and OCE-1635403) to R.C.Z. Metabolomics analyses and interpretation were conducted under the Laboratory Directed Research and Development (LDRD) Program at the Pacific Northwest National Laboratory (PNNL), a multi-program national laboratory operated by Battelle for the U.S. Department of Energy (DOE) under Contract DE-AC05-76RL01830. A portion of this research was also performed under the Facilities Integrating Collaborations for User Science (FICUS) initiative (#50358) and used resources at the Environmental Molecular Sciences Laboratory (EMSL), which is a DOE Office of Science User Facility. EMSL is sponsored by the DOE Office of Biological and Environmental Research and operated under contract DE-AC05-76RL01830.

Author contributions

R.C.Z., N.D.W. and C.Z.S. designed research. R.C.Z. and C.Z.S. maintained the experimental system, conducted growth measurements and collected all leaf samples. L.J.K. conducted sample processing. A.R.U. led the metabolomics sample analyses and data compilation. All of the authors participated in writing the paper.

Competing interests

The authors declare no competing interests.

Additional information

Supplementary information is available for this paper at <https://doi.org/10.1038/s41598-020-61684-x>.

Correspondence and requests for materials should be addressed to C.C.Z.-S.

Reprints and permissions information is available at www.nature.com/reprints.

Publisher's note Springer Nature remains neutral with regard to jurisdictional claims in published maps and institutional affiliations.



Open Access This article is licensed under a Creative Commons Attribution 4.0 International License, which permits use, sharing, adaptation, distribution and reproduction in any medium or format, as long as you give appropriate credit to the original author(s) and the source, provide a link to the Creative Commons license, and indicate if changes were made. The images or other third party material in this article are included in the article's Creative Commons license, unless indicated otherwise in a credit line to the material. If material is not included in the article's Creative Commons license and your intended use is not permitted by statutory regulation or exceeds the permitted use, you will need to obtain permission directly from the copyright holder. To view a copy of this license, visit <http://creativecommons.org/licenses/by/4.0/>.

© The Author(s) 2020